学　位　論　文

Studies on transmission dynamics of viral infectious disease by using mathematical model

(数理モデルを用いたウイルス感染症の感染動態に関する研究)

2022 年 3 月

北海道大学

坂本　洋平

Yohei Sakamoto

学　位　論　文

Studies on transmission dynamics of viral infectious disease by using mathematical model

(数理モデルを用いたウイルス感染症の感染動態に関する研究)

2022 年 3 月

北海道大学

坂本　洋平

Yohei Sakamoto

Contents

List of publications and presentations

Part of the research has been published as listed below:

1. Sakamoto Yohei, Takayuki Yamaguchi, Nao Yamamoto, Nishiura Hiroshi. Modeling the elevated risk of yellow fever among travelers visiting Brazil, 2018. Theoretical Biology and Medical Modeling. 2018;15(9).
2. Sakamoto Yohei, Nishiura Hiroshi. Time dependent risk of cytomegalovirus infection in Japan. Mathematical Biosciences and Engineering. 2019;16(5):4082-4091.

Abstract

【Background】

Mathematical models of infectious diseases are systems that can be used to mathematically represent and analyze the dynamics of infectious diseases in a population. In this study, the stability of the abovementioned models is analyzed and their validity quantitatively confirmed. It is discovered that mathematical models of infectious diseases are essential in infectious disease epidemiology. When constructing and analyzing mathematical models for individual infectious diseases, transmission characteristics must be clarified by considering factors such as the biological nature of the disease, clinical perspectives, human behavior, and individual heterogeneity. Developing the models from scratch for a wide range of infectious diseases will delay their implementation and result in their inability to model the spread of infection. Therefore, it is crucial to establish methodologies for each infectious disease using similar elements, and then adapt them promptly when an epidemic occurs. When using a mathematical model for viral infections, a model that considers factors such as drug treatment, diagnosis, surveillance, transmission route, and vaccine must be considered to estimate the number of potentially infected people as well as risks. In this study, two viral infections (cytomegalovirus and yellow fever) with different characteristics are formulated and their epidemic dynamics and risks quantitatively evaluated.

【Methods】

Chapter 1 (Cytomegalovirus):

Seroepidemiological datasets (i.e., the prevalence of anti- cytomegalovirus (CMV) IgG antibodies) for pregnant women obtained from five cord blood banks in Sapporo, Tokyo, Osaka/Kyoto, Okayama, and Fukuoka from 1996 to 2009 were used to quantify the time-dependent transmission dynamics of CMV infection in Japan. By employing a mathematical model and using the maternal age distribution of childbirths from the Vital Statistics of Japan, we computed seroprevalence among pregnant Japanese women as a function of time.

Chapter 2 (Yellow fever):

To estimate the risk of yellow fever among travelers, we analyzed both confirmed cases in Brazil and imported cases reported abroad (Chile, Argentina, the Netherlands, Switzerland, France, the

United Kingdom, Romania, and Germany) from May 2017 to May 2018. A statistical model was employed to capture the risk of importing yellow fever by returning international travelers from Brazil. We estimated the relative risk of importation among travelers by the extent of wealth measured based on the gross domestic product (GDP) per capita and the relative risk obtained by the random assignment of travelers' destinations within Brazil based on the relative population size.

【Results】

Chapter 1 (Cytomegalovirus)

Based on a total of 22,100 samples, 16,191 were identified as positive, with the sample proportion estimated to be 73.3% (95% CI: 72.7, 73.8). By linearly regressing the sample proportion by year, it was discovered that the seropositive fraction decreased by 0.7% annually ($p < 0.001$). From 1980–2009, the median age of infection increased from 10.0 to 19.7 years old. However, the force of infection, i.e., the rate at which susceptible individuals are infected, decreased from 0.04 to 0.03 (/year) over the period from 1996 to 2009. Whereas the total number of births in Japan declined steadily, the estimated number of live births at risk of CMV infection increased over time. Comparing the time-dependent patterns of the estimated force of infection against the different geographic locations of cord blood banks in Japan, whereas a time-dependent decline was evident in Hokkaido and Fukuoka, the rate of decrease in the force of infection was lower in Tokyo.

Chapter 2 (Yellow fever)

Travelers from the wealthier fraction of countries were a = 2.3 (95% confidence interval, CI: 0.7, 8.6) times more likely to be infected with yellow fever than those from countries below the median GDP per capita. The upper-half of wealthier countries indicated 2.1–3.4 times greater risk of importation than the remainder. Among countries in the lower half of the GDP per capita, the risk of importation was 2.5–2.8 times greater as compared with the risk of travelers' infection within Brazil determined based on the regional population size.

【Discussion】

Chapter 1 (Cytomegalovirus)

We show that the force of infection for CMV in Japan declined over time using blood samples from pregnant women only. Our data revealed that in 2009, at least 0.3 million women in Japan may have been at risk of contracting a CMV infection during the perinatal period. Moreover, approximately 2,726 congenital CMV infections were expected to have occurred in 2009. The average age at infection has already reached the childbearing age. It is noteworthy that the age at infection can increase to approximately 30 years, which is the ongoing mean age at child delivery. Furthermore, if vaccination can be implemented for controlling CMV in the future, then the age at infection may be further increased, which may coincide with the further elevation of age at delivery in Japan.

Chapter 2 (Yellow fever)

In this study, we show that countries with a higher GDP per capita are infected the most frequently, which indicates that travelers' local destination and behavior are likely to be key determinants of the heterogeneous risk of importing cases. In addition, we discovered that non-wealthy countries indicated 2.5–2.8 times greater risk of importing yellow fever cases compared with the typical modeling assumption that the destination-specific risk of infection is proportional to the population size of the destination relative to the entire country. This study exhibited four limitations: First, the notification of yellow fever cases was biased by the extent of the ascertainment. Second, the spatial risk of infection could not be considered on a finer scale. Third, vaccination coverage among travelers from countries without routine yellow fever immunization was assumed to be proportional to the GDP per capita. Fourth, the lower confidence bound of our relative risk estimates was less than one, and the sample size was not substantial. The abovementioned limitations must be addressed in future studies to achieve a finer estimation of the infection risk among travelers. However, in our current study, we successfully quantified the relative risk of infection by GDP per capita and then compared it with the risk based on population-size-specific assumptions of travelers' destinations.

【Conclusion】

Chapter 1 (Cytomegalovirus)

Data from the seroprevalence survey among pregnant women were analyzed as a function of time, and the seropositivity among pregnant women was calculated based on year. By fitting the

computed probability to the observed seropositive data, we show that the observed decline in the proportion of CMV-positive pregnant women mirrored the steadily declining force of infection over time. Owing to the elevated age at infection, pregnant women are exposed to a high risk of congenital CMV infections in Japan.

Chapter 2 (Yellow fever)

Travelers from wealthier countries are at an elevated risk of yellow fever, thereby allowing us to speculate that travelers' local destination and behavior are likely to be key determinants of the heterogeneous risk of importation. Travelers must be informed of the ongoing geographic foci of transmission. If visits to tourist destinations with a history of imported cases are inevitable, then travelers are urged to receive vaccination in advance.

List of Abbreviations

AIDS	Acquired immunodeficiency syndrome
ART	Antiretroviral therapy
CFR	Case fatality risk
CI	Confidence intervals
CMV	Cytomegalovirus
COVID-19	Coronavirus disease 2019
EIA	Enzyme immunoassay
FOI	Force of infection
GDP	Gross Domestic Product
HBV	Hepatitis b virus
HIV	Human immunodeficiency virus
MHLW	Ministry of Health, Labour and Welfare, Japan
PAHO	Pan American Health Organization
PCR	Polymerase chain reaction
R_0	Basic reproduction number
SARS	Severe acute respiratory syndrome
UNWTO	World Tourism Organization
WHO	World Health Organization

Introduction

Mathematical models of infectious diseases are systems that can be used to mathematically represent and analyze the dynamics of infectious diseases in a population. The mathematical model of infectious diseases originated from smallpox research in the 18th century, and the basic reproduction number (R0), which is the basic indicator in infectious disease epidemiology, emerged in the latter half of the 19th century. In the 20th century, the discovery of the transmission threshold of the malaria epidemic and the development of differential equation models provided a foundation for establishing a mathematical model of infectious diseases. Subsequently, stability analysis was performed, quantitative validity was gradually assured, and mathematical models of infectious diseases became essential in infectious disease epidemiology (Dietz 1988; Dietz and Heesterbeek 2002; Kermack and McKendrick 1927; Anderson and May 1991). Currently, mathematical modeling of infectious diseases has progressed significantly owing to innovations in statistical estimation (e.g., Markov chain Monte Carlo methods), increased computational power of computers, and electronic and online management of clinical, epidemiological, genetic, and other biological information. Mathematical models of infectious diseases have been applied to the objective analysis and prediction of the prevalence of specific infectious diseases; additionally, they have become an essential method in health and medical policy-making, such as vaccination strategies (Glasser 2004).

Mathematical models of infectious diseases integrate mathematical models with statistical methods for parameter estimation and hypothesis testing by fitting actual data to the constructed models. When constructing and analyzing mathematical models for individual infectious diseases, transmission characteristics must be clarified by considering factors such as the biological nature of the disease, clinical perspectives, human behavior, and individual heterogeneity. Because available data are often insufficient, a mathematical hypothesis and a strategy must be developed for future data acquisition. However, the model implementation will be delayed, which will result in the inability to model the spread of infection if the models are developed from scratch for a wide range of infectious diseases. Therefore, it is crucial to establish methodologies for each infectious disease with similar elements, and then adapt them promptly when an epidemic occurs.

Many viral infections, such as the human immunodeficiency virus disease (HIV)/acquired immunodeficiency syndrome), severe acute respiratory syndrome (SARS), highly pathogenic avian influenza H5N1, influenza H1N1-2009, Zika fever, Ebola hemorrhagic fever, and coronavirus disease 2019 (COVID-19) have become public health problems in recent years. In public health, several problems exist in controlling viral infections. Whereas most bacterial infections can be treated using antimicrobial agents, viral infections can only be treated using antiviral agents for selected viruses, such as hepatitis B, HIV, and influenza. In addition, except for diseases for which antigen and antibody tests have been established, polymerase chain reaction and viral culture are often required for a definitive diagnosis, which are difficult to perform in clinical settings owing to economic and personnel reasons. For the same reason, adequate surveillance is often not performed. When using a mathematical model for viral infections, a model that considers factors such as drug treatment, diagnosis, surveillance, transmission route, and vaccine must be considered to estimate the number of potentially infected people and risks.

In this study, two viral infections with different characteristics were formulated and their epidemic dynamics and risks quantitatively evaluated. Chapter 1 provides an assessment of the risk of cytomegalovirus (CMV), which can cause congenital diseases when transmitted from a mother to a child. Chapter 2 presents an evaluation of the risk of yellow fever as a vaccine-preventable travel infectious disease.

Chapter 1　Time-dependent risk of cytomegalovirus infection in Japan

Introduction

Cytomegalovirus (CMV) is a double-stranded DNA virus belonging to Betaherpesvirinae. CMV infections occur primarily during infancy or adolescence, and a substantial fraction of these infections are asymptomatic. As observed in infections involving other herpesviruses, latent infection can continue over a person's lifetime. Infections can cause infectious mononucleosis and hepatitis, including among immunocompetent individuals (Kenneson and Cannon, 2007). Premature babies and patients with primary immunodeficiency disease who have undergone transplantation or have acquired immunodeficiency syndrome are particularly susceptible to viral reactivation, which can trigger opportunistic infections, such as retinitis, pneumonia, hepatitis, and myocarditis (Kenneson and Cannon, 2007).

Once CMV infection or reactivation occurs in a pregnant woman, the virus is transferred from the mother to the fetus through the placenta with high probability, thereby resulting in congenital CMV infection. It has been estimated that 1%–4% of antibody-negative pregnant women experience their first CMV infection during pregnancy, and that 33%–40% of infections in these seronegative women involve their fetus (Stagno and Whitley, 1985). Some of these fetal infections (10%–15%) are clinically relevant, as revealed by low birth weight, premature birth, jaundice, purple skin splotches and/or rash, hepatosplenomegaly, and thrombocytopenia (Stagno and Whitley, 1985). Moreover, 90% of clinically relevant congenital CMV infections and 10%–15% of asymptomatic congenital infections involve sequelae (after effects), including neurological abnormalities such as hearing loss, mental retardation, and visual disability (Stagno and Whitley, 1985; Ogawa et al, 2007). Hearing loss is characteristic of CMV infections, and it constitutes 15% of all cases of severe hearing loss at the minimum (Ogawa et al, 2007).

The frequency of post-infection disability attributable to congenital CMV infection is estimated to be 10 among 10,000 live births in Japan (Azuma et al, 2010; Taniguchi et al, 2014; Hirota, 1992), a rate comparable to the frequency of trisomy 21 (i.e., Down syndrome), which is estimated to be 9.6 per 10,000 births. Nevertheless, the infection is primarily asymptomatic; this implies that its timely laboratory testing is difficult, and few methods exist that can confirm the causality of any apparent disability originating from CMV infection. Hence, a substantial number

of CMV-associated disabilities have been overlooked. Considering that the transmission of CMV is potentially associated with socioeconomic status (Dowd et al, 2009), epidemiological monitoring of the frequency of infection and its variations as a function of time due to time-varying economy is critical.

Recently, a decline in the proportion of people who are CMV antibody-positive has been observed in several countries, including Japan (Azuma et al, 2010, Taniguchi et al, 2014; Almeida et al, 2001; Colugnati et al, 2007; Fang et al, 2009; Griffiths et al, 2001). This decline implies that the risk of congenital infection may have increased among women of childbearing age. Paradoxically, the decline in the force of infection may render pregnant women, who are supposed to be immune to CMV, susceptible to primary infection during pregnancy owing to the reduced frequency of infection during childhood. To obtain more information regarding this phenomenon, the time-dependent transmission dynamics of CMV infection in Japan was quantified in this study by analyzing seroepidemiological datasets for pregnant women.

Materials and Methods

Epidemiological data

Published seroepidemiological data obtained from 1996 to 2009 in Japan were used in the present study (Azuma et al, 2010). The prevalence of anti-CMV IgG antibodies was assayed using serum samples from five cord-blood banks in Sapporo, Tokyo, Osaka/Kyoto, Okayama, and Fukuoka. Maternal serum samples were obtained from pregnant women who agreed to store their cord blood prior to delivery or operation, and maternal serum samples were examined for antibody prevalence. From 1996 to 2007, the particle agglutination method was employed to measure anti-CMV IgG antibodies, except in Kyoto and Sapporo, where the enzyme immunoassay (EIA) method was employed until 2002, after which it was replaced by microparticle EIA from 2003 to 2007. In 2008 and 2009, all sites were analyzed using chemiluminescence EIA. A total of 22,100 serum samples were examined (Azuma et al, 2010). The ages of the sampled mothers were not available. However, the mothers' age at delivery can be obtained from the annual census of Japan. Hence, in addition to the seroprevalence data, we extracted the maternal age distribution for childbirth from 1996 to 2009 from the Vital Statistics of Japan (Ministry of Health, Labour and Welfare, Japan (MHLW), 1980-2009).

Mathematical model

The observed seropositive fraction represents the maternal antibody data as a function of time. In this study, we employed a mathematical model to capture the time-dependent transmission dynamics of CMV from seroprevalence data. Let $S(a, t)$ be the fraction of susceptible individuals at age a and year t. Assuming that every individual is susceptible to CMV and by disregarding maternal antibodies, we have the boundary condition $S(0,t) = 1$ for any t. Using the force of infection $\lambda(a, t)$, i.e., the rate at which susceptible individuals experience infection, which depends on age a and year t, the susceptible individuals are reduced, as follows:

$$\left(\frac{\partial}{\partial a}+\frac{\partial}{\partial t}\right)S(a,t) = -\lambda(a,t)S(a,t) \tag{1}$$

The force of infection is typically modeled as a function of the prevalence of infection in the population. We do not decompose the force of infection but assume that the force of infection can vary with time and age. Namely, we assume that the force of infection is separable into age and time components and that the force of infection is age independent, as is assumed in the tuberculosis model (Rieder, 2005), i.e.,

$$\lambda(a,t) = f(a)\lambda(t) \tag{2}$$

Moreover,

$$\lambda(0,t-a) = \lambda(a,t-a) = \lambda(t-a) \tag{3}$$

Namely, $\lambda(a,t) = \lambda(t)$. Integrating both sides of Eq. (1), we obtain

$$S(a,t) = S(0,t-a)\exp\left(-\int_{t-a}^{t}\lambda(s)\,ds\right) = \exp\left(-\int_{t-a}^{t}\lambda(s)\,ds\right) \tag{4}$$

Parametrically modelling $\lambda(t)$ as an exponentially decreasing function with year t, i.e., $\lambda(t) = \lambda_0 exp(-\beta t)$, we have

$$S(a,t) = \exp\left(-\int_{t-a}^{t}\lambda_0\exp(-\beta s)\,ds\right), \tag{5}$$

where λ_0 and β are parameters to be estimated. Let $b(a,t)$ be the relative frequency of live births as a function of age a in year t. The expected probability of seropositivity is modeled as

$$p(t) = \int_0^{\infty} b(a,t)\{1 - S(a,t)\}\, da \tag{6}$$

in year *t*.

To quantify the force of infection, a likelihood-based approach is employed. For m_t positive women among the total serum samples obtained from n_t women in year *t*, the likelihood function for estimating parameter θ is modeled as

$$L(\theta: \boldsymbol{n}, \boldsymbol{m}) = \prod_{t=1996}^{2009} \binom{n_t}{m_t} p(t - t_0)^{m_t} \big(1 - p(t - t_0)\big)^{n_t - m_t} \tag{7}$$

The t_0 is set to 1950 as the starting point for calendar time. The 95% confidence intervals (CIs) are computed using the full likelihood. In the sensitivity analysis, not only the entire Japan estimate but also the force of infection is estimated based on the geographic location of the cord blood bank.

Once the unknown parameters are estimated, the mothers at risk of infection in year *t* is calculated as follows:

$$B(t) \int_0^{\infty} b(a,t) S(a,t)\, da, \tag{8}$$

where *B*(*t*) represents the total number of live births in year *t.* Similarly, the expected number of live births with CMV infection, *q*(*t*), is calculated as follows:

$$q(t) = B(t) \int_0^{\infty} b(a,t) S(a,t) \left\{1 - \exp\left(-\int_{t-\theta}^{t} \lambda_0 \exp(-\beta s)\, ds\right)\right\} da, \tag{9}$$

where θ is the gestational week in a year at risk of congenital CMV infection, which was assumed to be 16/52 in this study.

Results

Based on 22,100 samples, 16,191 were identified as positive, with the sample proportion estimated to be 73.3% (95% CI: 72.7, 73.8). As a function of time, the highest proportion of positive cases was estimated to be 82.5% in 1996 and the lowest to be 70.3% in 2004. Figure 1A shows the observed sample proportion as a function of time. By linearly regressing the sample

proportion by year, the seropositive fraction appeared to have decreased annually by 0.7% ($p < 0.001$).

The assumed parametric function for the force of infection, i.e., $\lambda(t) = \lambda_0 exp(-\beta t)$, captures the approximate observed time trend for the seropositive fraction (Figure 1A). λ_0 was estimated to be 0.15 (95% CI: 0.10, 0.20), and the exponential decrease rate β was 0.024 (95% CI: 0.017, 0.030). Figure 1B shows the reconstructed force (hazard) of infection among the susceptible individuals by year. A monotonically decreasing trend was observed in the force of infection, and a decrease of 0.04 to 0.03 per year from 1996 to 2009 was observed. In a stationary population, a decline indicates that the average age at infection is elevated from 1/0.04 = 25.0 years to 1/0.03 = 33.3 years during the study period.

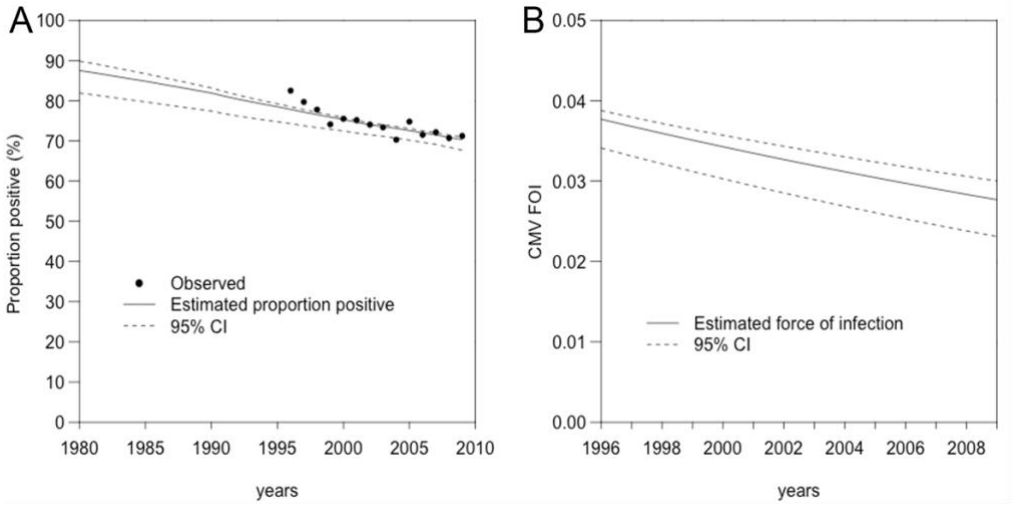

Figure 1. Seroepidemiological trends in anti-cytomegalovirus (CMV) antibodies among pregnant women in Japan over time. A. Observed (dot) and estimated (line) proportion of pregnant women positive for cytomegalovirus (CMV)-IgG antibodies in Japan. Black dots represent observed proportions from 1996 to 2009. Solid line represents estimated proportion from 1980 to 2009, with upper and lower 95% confidence intervals shown as dashed lines. B. Estimated force of infection (FOI) for CMV in Japan. Two dashed lines represent upper and lower 95% confidence intervals as computed based on profile likelihood. Annual CMV FOI (vertical axis unit) is shown.

Figure 2A shows the age-specific immune fractions for people by year (1980, 1990, 2000, and 2009). A rightward shift was observed in the age-dependent seroprevalence curve, which reflected a time-dependent decline in the force of infection. In the period from 1980 to 2009, the median age of infection was elevated from 10.0 to 19.7 years. This delay in infection was overlaid with a delay in childbirth age, as shown in Figure 2A. In the period from 1980 to 2009, the mode for the maternal age of live births increased from 26 to 29 years. Would this age shift prevent an increased risk of CMV infection among pregnant women? The answer is no, as shown in Figure 2B. Whereas the total number of births has declined steadily in Japan, the estimated number of live births at risk of CMV infection increased over time. In 2009, at least 0.3 million women were considered to have been at risk of CMV infection during the perinatal period. In 1996, the estimated number of pregnant women at risk was 268,000, but the figure increased continuously over time. The estimated total number of congenital CMV infection events was 3,124 in 1996, which decreased to 2,726 in 2009.

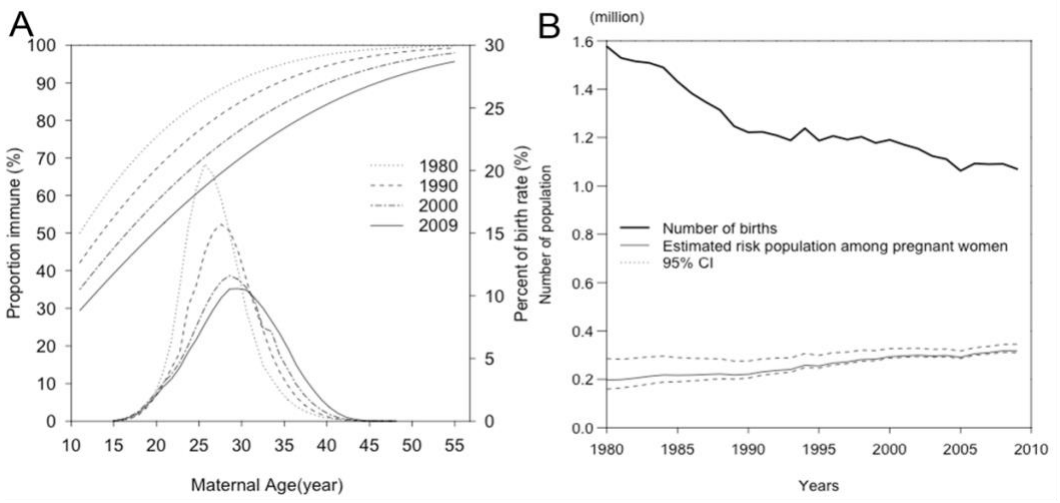

Figure 2. Estimated populations at risk of CMV infection in Japan. A. Comparison of age-specific frequency of live births and age-dependent proportion of immune individuals. Using time-dependent force of infection mathematical modelling described in Methods section, immune fraction was computed for years 1980, 1990, 2000, and 2009. B. Comparison of time trends between total number of live births (bold line) and number of live births at risk of contracting CMV infection. Solid line represents maximum-likelihood estimate, and dashed lines represent lower and upper 95% confidence intervals (CIs), as computed using bootstrap method.

Figure 3 shows a comparison of the time-dependent patterns of the estimated force of infection against the different geographic locations of cord blood banks in Japan. Although a time-dependent decline was observed in Hokkaido and Fukuoka, the decline rate of the force of infection was lower in Tokyo. The estimates varied widely depending on the geographic location. The increased range of the force of infection in 2009, as compared with those in earlier years, indicates that geographic heterogeneity has likely increased.

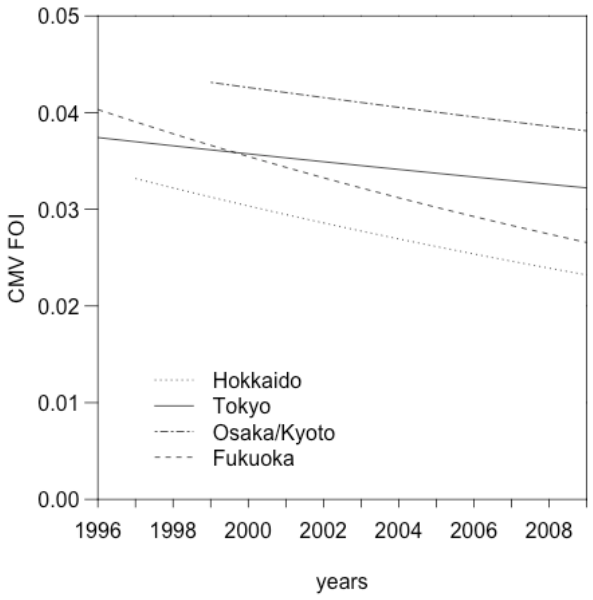

Figure 3. Force of infection (FOI) comparison for CMV in multiple Japanese cities from 1996 to 2009. Maximum-likelihood estimates for Hokkaido, Tokyo, Osaka/Kyoto, and Fukuoka are compared. Annual CMV FOI (vertical axis unit) is shown.

Discussion

In the present study, the time trend for the force of infection in Japan was examined by analyzing the seroprevalence survey data from pregnant women as a function of time. By employing a mathematical model and using the maternal age distribution of childbirth from Japanese vital statistics, we computed the probability of seropositivity among pregnant women by year. By fitting the computed probability to the observed seropositive data, we showed that the observed decline in the proportion of CMV-positive pregnant women mirrored the steadily declining force of infection over time.

To the best of our knowledge, the present study is the first to demonstrate the decline in the prevalence of CMV infection over time in Japan. Notably, the estimate was obtained using data from blood samples from pregnant women only. Numerous published epidemiological studies indicated that the seroepidemiological characteristics of CMV have changed over time and age (e.g., studies in the USA (Colugnati et al, 2007) and China (Fang et al, 2009), and a mathematical modeling study that investigated the risk of infection at the population level in Brazil (Almeida et al, 2001)). A possible age shift for CMV infection was discussed in some modeling studies (Almeida et al, 2001; Fang et al, 2009), including those focusing on future vaccination against the disease (Almeida et al, 2001; Hogea et al, 2015; Lanzieri et al, 2014; Azevedo and Amaku, 2011). Our study results enrich the literature by demonstrating that the age at which CMV infection is acquired increased naturally over time, a trend that we successfully reconstructed using serum samples from pregnant women only. The exact reasons for this decline remain ambiguous; however, considering that CMV is transmitted through direct contact and via the environment, reduced physical contact over time and improved hygienic conditions may contribute to the observed phenomena. Although regional variations were reflective of sampling errors, the slower infection decline in Tokyo compared with the other three cities is consistent with the notion of improved hygiene. Compared with other cities, Tokyo has been urbanized for a longer period.

We focused on the fact that the age at childbirth has increased over time, in addition to a monotonic decline in the total number of live births (Vyse et al, 2009). Despite the declining birth rate, we demonstrated that the age of CMV infection has increased over time, in addition to

the population size of women at risk of CMV infection. In fact, as many as 0.3 million newborn in Japan each year will be susceptible to CMV infection during the perinatal period, indicating the importance of continuous age of infection monitoring based on the childbearing age of women. The average age at infection has reached the childbearing age. It is noteworthy that the age at infection can increase further to approximately 30 years, which is the ongoing mean age at child delivery. Additionally, vaccination can results in a further increase in the age at infection.

Our study exhibited some limitations. First, we employed an age-independent assumption for the force of infection, which was necessary because the empirical data did not provide any information regarding the age element. We adjusted the age-dependent frequency of childbirth explicitly because, in this context, age was considered an important element for regulating the transmission dynamics of CMV (Boven et al, 2017). Continual monitoring of pregnant women and stratifying them into multiple age groups would allow for a more accurate estimation in future studies. Second, an exponential model was employed to parametrically capture the time trend of the force of infection. As shown in Figure 1A, we could not obtain any additional insight (e.g., more detailed parametric functions) from the data pertaining to the time-dependent element. Hence, observations for a longer period are required. Third, the anti-CMV IgG assay results were based on different laboratory testing procedures from 1996 to 2007; however, we analyzed the data collectively because we did not identify any considerable differences in the observed seroprevalence values arising from the different testing methods. However, in the sensitivity analysis, we successfully examined the geographic heterogeneity in the force of infection. Fourth, the fixed cut-offs used in serological assays might have resulted in the underestimation of seropositive individuals. As indicated previously, although a fixed cut-off can ensure a high sensitivity, specificity might be sacrificed (Kafatos et al., 2016).

Considering that the force of infection declined naturally, the effect of introducing mass vaccination to children and women for targeted vaccination policies on the outcome of overall infections and congenital CMV infections should be investigated based on different settings for both CMV (Hogea et al, 2015; Lanzieri et al, 2014; Azevedo and Amaku, 2011) and other infectious diseases (Mossong et al, 2004; Mossong et al, 2008; Fernandes et al, 2009; Bollaerts et

al, 2017). Reconstructing the time- and age-specific patterns for immune individuals in the population would facilitate the design of an object-oriented vaccination program.

Acknowledgements

HN received funding support from the Japan Agency for Medical Research and Development (JP18fk0108050), Japan Society for the Promotion of Science KAKENHI (Grant Numbers 16KT0130, 17H04701, 17H05808, and 18H04895), Health and Labour Sciences Research Grant (H28-AIDS-General-001), Inamori Foundation, Telecommunication Advancement Foundation, and Japan Science and Technology Agency (JST) CREST program (JPMJCR1413). The funders did not participate in the study design, data collection and analysis, decision to publish, or manuscript preparation.

Chapter 1 was originally published in

Sakamoto Yohei, Nishiura Hiroshi. Time-dependent risk of cytomegalovirus infection in Japan Mathematical Biosciences and Engineering 2019;16(5):4082-4091.

Chapter 2 Elevated risk modeling of yellow fever among travelers visiting Brazil in 2018

Introduction

Yellow fever virus (Flavivirus) causes yellow fever, which is transmitted human to human via the Aedes mosquito species (Monath, 2001). In addition to the human–mosquito–human transmission cycle, nonhuman primates can be infected with the virus, and such a transmission cycle has been reported to be the cause of continued transmission in Brazil (Dexheimer et al, 2018; Fernandes et al, 2017; Moreira-Soto et al, 2018). Exposure to this virus primarily results in asymptomatic infection; however, some patients develop fever, headache, chills, muscle pain, nausea, and vomiting following an incubation period of 3–6 days (Monath, 2001). If exacerbated, the case fatality risk (CFR) of a severe clinical disease is 47% (i.e., from 40% to 80% (Johansson et al, 2014)), and no specific treatment is available. In this regard, immunization is the mainstream countermeasure (Wisseman et al, 1962). Residents of high-risk areas and travelers visiting those areas are advised to be vaccinated.

The yellow fever epidemic in Brazil from December 2016 to June 2017 involved 777 confirmed cases among Brazilian residents, and the CFR was estimated to be 34%, with 261 deaths (Pan American Health Organization (PAHO), 2018). Whereas the end of the epidemic was declared in September 2017, sporadic cases continued, and a surge of cases began in December 2017 (World Health Organization (WHO), 2018). On January 16, 2018, the World Health Organization recognized the ongoing epidemic and recommended vaccination among all residents of Rio de Janeiro and São Paulo, and a vaccination campaign targeting Bahia, Rio de Janeiro, and São Paulo was ordered by the government of Brazil (World Health Organization (WHO), 2018a). As of June 8 2018, 1257 confirmed cases and 394 deaths have been reported (Ministerio da Saude, Brazil, 2018).

Whereas no imported cases were reported during the epidemic from 2016 to 17, multiple importation events were reported during the epidemic from 2017 to 18. As of June 8, 2018, 12 imported cases have been reported in eight different countries since December 2017 (Ministerio da Saude, Brazil, 2018; Gossner et al, 2018). To observe multiple importation events, the epidemic in 2017–2018 that involved Rio de Janeiro and São Paulo can be analyzed since it

comprised more cases than those in 2016–2017 (Possas et al, 2018). The aim of this study was to quantify the risk of infection among travelers visiting Brazil in 2018.

Materials and Methods

Epidemiological data

To estimate the risk of yellow fever among travelers, we analyzed both confirmed cases in Brazil from 2017 to 2018 (Ministerio da Saude, Brazil, 2018) and imported cases reported abroad. As of May 8, 2018, three imported cases were reported from Chile, three from Argentina, and one each from the Netherlands, Switzerland, France, the United Kingdom, Romania, and Germany respectively(World Health Organization (WHO), 2018b; World Health Organization (WHO), 2018c; Gossner et al, 2018; Weigand, 2018). The imported cases involved the citizens of the reported countries, and they were regarded as imported owing to travel to Brazil. Except for cases from the Netherlands and France and one case in Argentina, the imported cases involved a history of visits to Ilha Grande, municipality of Angra do Reis, State of Rio de Janeiro, Brazil (WHO, 2018b).

Mathematical model

To calculate the expected risk of importation, the inbound travel volume c_i from each country i to Brazil was retrieved from the World Tourism Organization (UNWTO, 2017). In addition, we used the relative value of the gross domestic product (GDP) per capita, g_i, of country i, which was normalized by the maximum GDP in 2016 for imputation of vaccination coverage (see below) (Central Intelligence Agency, 2017). This imputation was validated partially via a statistical analysis of the association between GDP per capita and importation risk by country. After confirming that the variance between the two groups was not significantly different via the F-test, we employed the Student's t-test to compare the GDP per capita between countries with and without imported cases. Moreover, the vaccination coverage v_i of country i in 2015 was retrieved partially from a published study (Shearer et al, 2017).

Following Dorigatti et al. (Dorigatti et al, 2017), we modeled the expected number $E(c_i)$ of imported yellow fever cases c_i in country i as follows:

$$E(c_i) = n_i(1 - v_i)q_i \frac{pop_s}{pop_b} \frac{c_s}{pop_s} \frac{\mu_E + \mu_I}{w} \sum_{s=1}^{12} f_s p_s, \quad (10)$$

where n_i is the yearly inbound number of travelers visiting Brazil from country i; v_i is the vaccination coverage; q_i represents the relative risk of infection among travelers from country i, which we would like to estimate; pop_s and pop_b represent the population sizes of the three major states of the 2017–2018 epidemic (Minas Gerais, Rio de Janeiro, and São Paulo) and the entire Brazilian population, respectively (pop_s = 81,230,574 and pop_b = 202,768,562). The number of confirmed yellow fever cases in the affected states is denoted as c_s. We did not use the undiagnosed factor of 10, which was adopted elsewhere (Johansson et al, 2014; Dorigatti et al, 2017), because we estimated the expected number of confirmed imported cases abroad. w is the mean length of stay in Brazil (w = 17 days); f_s and P_s are the normalized monthly frequency of cases and volume of travelers in month s, respectively (fs from December 2017 to March 2018 accounted for 98.4%, and P_s during the same period was 47.6% of the total). Although not specified in Eq. (10), month s was integrated from December 2017 to March 16, 2018, and censoring in March was incorporated by accounting for the number of days (16/31). μ_E and μ_I represent the mean latent and infectious periods, respectively, assumed as 4.6 be 4.5 days, respectively. It is noteworthy that Eqs. (10) is intact, including when the unascertained/asymptomatic fraction of cases is considered. Assuming that the confirmation probability among all infected individuals is α, both sides of Eq. (10) are divided by α to express all terms as the total number of infected individuals, and the constant $1/\alpha$ is cancelled out from both sides.

Unlike some previous calculations (Dorigatti et al, 2017; Tsuzuki et al, 2017), we disregarded the stochasticity of the lengths of latent and infectious periods for simplicity. We define

$$m_i(q_i) := \frac{E(c_i; q_i)}{1 - v_i} \quad (11)$$

Subsequently, we employ the zero-inflated Poisson distribution to describe the observed frequency of imported cases in country i, as follows:

$$h(X=j;q_i)=\begin{cases} v_i+(1-v_i)exp\big(-m_i(q_i)\big), & if\ j=0 \\ (1-v_i)\dfrac{exp\big(-m_i(q_i)\big)m_i(q_i)^j}{j!}, & if\ j>0 \end{cases} \quad (12)$$

The mean number of imported cases based on Eqs. (12) is expressed as $E(c_i) = (1 - v_i)\, m_i\, (q_i)$. With respect to vaccination coverage v_i among travelers from country *i*, we model it as

$$v_i=\begin{cases} u_i, & \text{if vaccination coverage available} \\ \dfrac{k}{1+exp(-g_i)}, & \text{if vaccination coverage is unavailable} \end{cases} \quad (13)$$

We adopted the logit transformation because it does not require additional parameters. The estimated vaccine coverage in some routinely immunized countries is available in a published study (Shearer et al, 2017). Countries with known vaccination coverage include Trinidad and Tobago, Panama, Argentina, Colombia, Suriname, Peru, Venezuela, Ecuador, Paraguay, Guyana, Bolivia, Angola, Nigeria, Ghana, and Kenya. When information regarding vaccination coverage was unavailable, we extrapolated the vaccination coverage in country *i*. Considering that only a small fraction of travelers are vaccinated in those countries, *k* was assumed to be 0.10, which is the carrying capacity of the logistic distribution and is practically interpreted as the theoretical maximum of the vaccination coverage. g_i is the relative GDP per capita of country *i* compared with the country with the highest GDP per capita, as stated above. For the second case in Eq. (13), i.e., when vaccination coverage is unavailable, we imposed the assumption that, if no routine immunization is implemented, then a maximum of 10% of travelers visiting Brazil will have received vaccination, and that the coverage reflects a logit transformation of the relative GDP per capita. As the ceiling of coverage *k* is an influential parameter, we varied it from 0.01 (1%) to 0.90 (90%) in the sensitivity analysis.

We estimated q_i by the list of countries, i.e., by the first- and second-half of GDP per capita, because the propensity to visit high-risk areas of infection, which coincided with a resort area in the ongoing epidemic (Gossner et al., 2018; World Health Organization [WHO], 2018b), might vary with the extent of wealth of that particular country. q_i is modeled as

$$q_i = \begin{cases} aq, & \text{if GDP } \textit{per capita} \text{ of country } i \text{ is higher than median} \\ q, & \text{if GDP } \textit{per capita} \text{ of country } i \text{ is lower than median} \end{cases}, \quad (14)$$

where q is the relative risk of infection among travelers visiting from countries with the second-half of the GDP per capita, as compared with that from the assumption that the travelers' destination is randomly determined based on the regional population size of Brazil. Meanwhile, a is the relative risk of importing yellow fever among wealthier countries compared with the remainder with risk q.

For the observed counts of imported cases, **c**, written as a vector representing the input from all countries at risk of infection, the maximum likelihood estimates of a and q were obtained by minimizing the negative logarithm of the following likelihood:

$$L(a, q; \mathbf{c}) = \prod_i h(c_i) \quad (15)$$

The 95% confidence intervals (CIs) were computed using the profile likelihood.

Results

Figure 4 shows the curve of the 2017–2018 epidemic in Brazil as a function of the report week (Ministerio da Saude, Brazil, 2018). The highest incidence was reported in Week 3 of 2018, followed by a monotonic decline in incidence. Subsequently, the incidence declined significantly by Week 17, 2018. Figure 5 shows a comparison of GDP per capita by country with and without imported cases. The GDP per capita of countries with imported cases (n = 8) was 40,213 US dollars (95% CI: 25,614, 54,811), whereas that of countries without imported cases and with direct flight links from Brazil (n = 78) was 26,368 US dollars (95% CI: 21,593, 31,043). It was observed that the GDP per capita of countries with imported cases was significantly greater than those without (t = 2.34, p = 0.04, Student's t-test).

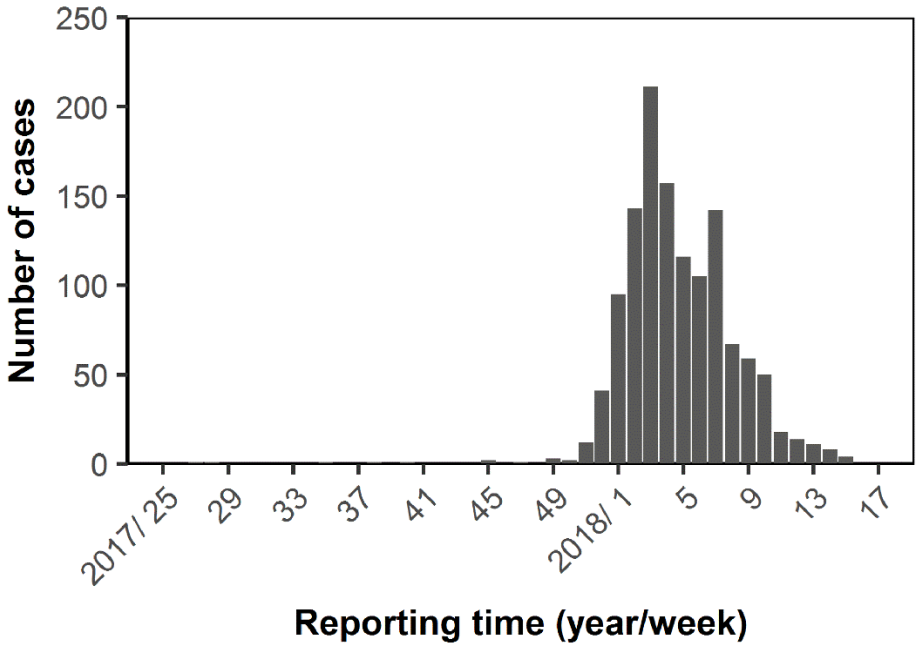

Figure 4. Weekly incidence of yellow fever cases in Brazil from 2017 to 2018. Weekly count of confirmed cases displayed as a function of report week (Ministerio da Saude, Brazil, 2018). Highest incidence was reported on Week 3 of 2018.

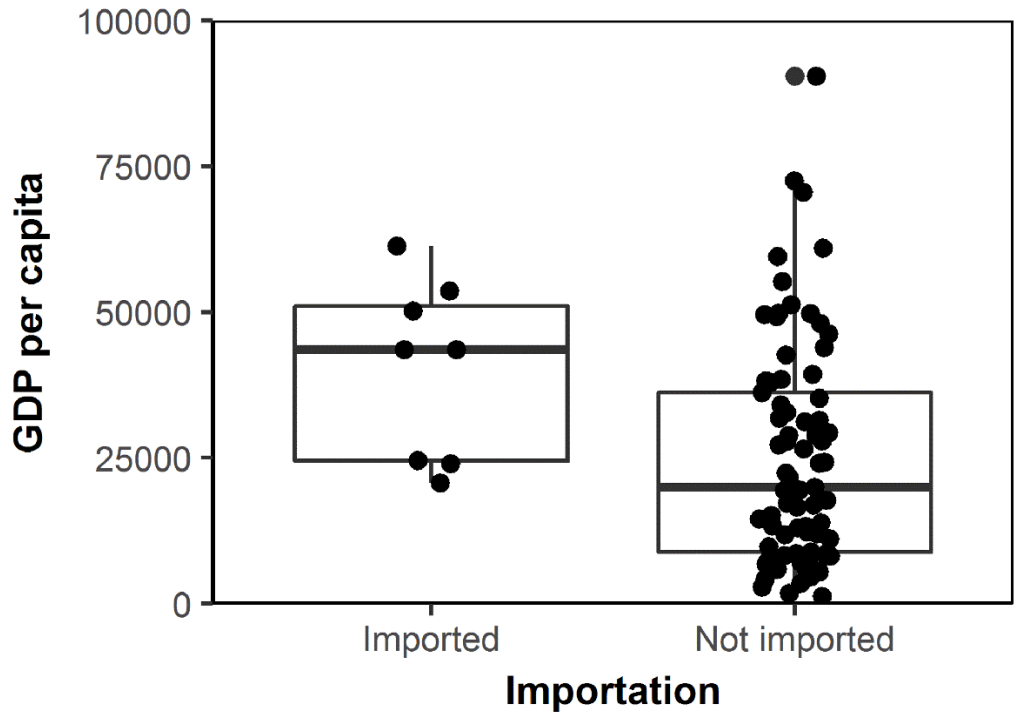

Figure 5. Comparison of gross domestic product (GDP) per capita by importation of yellow fever during 2017–2018 epidemic (*n* = 86).
GDP per capita is compared between countries with and without imported cases (*n* = 8 and 78, respectively) in our analysis. Bold mid-line in hinges represents median value. Lower and upper hinges correspond to first and third quartiles, respectively. Upper whisker extends from hinge to highest value that does not exceed 1.5 times the interquartile range; lower whisker extends from hinge to smallest value that does not exceed 1.5 times the interquartile range.

A total of 12 imported cases were reported in 8 different countries (Fig. 6a). The remaining 78 countries with inbound data for Brazil were included in the analysis. The known vaccinated fractions were as follows: Trinidad and Tobago (0.96), Panama (0.73), Argentina (0.94), Colombia (0.91), Suriname (0.89), Peru (0.90), Venezuela (0.87), Ecuador (0.78), Paraguay (0.80), Guyana (0.95), Bolivia (0.89), Angola (0.80), Nigeria (0.74), Ghana (0.89), and Kenya (0.78). Assuming k = 0.10, travelers from the wealthier fraction of countries were a = 2.3 (95% CI: 0.7, 8.6) times more likely to be infected with yellow fever compared with those from countries whose GDP per capita was below the median. Compared with the assumption that the risk of infection was governed by the population size of the epidemic location (i.e., three states with a substantial number of cases) relative to the entire Brazilian population ((i.e., Eq. (10) with q = 1.0) (Central Intelligence Agency, 2017), countries whose GDP per capita was below the median indicated q = 2.5 (95% CI: 0.8, 5.9) times greater risk of yellow fever.

Figure 6b shows the results of the sensitivity analysis. Varying an uncertain parameter k, i.e., the possible maximum value of the vaccination coverage among travelers from countries without routine immunization against yellow fever, did not significantly affect the estimated q_i. The relative risk of yellow fever among wealthier countries compared with countries with the second-half of GDP per capita ranged from 2.1 (with k = 0.01) to 3.4 (with k = 0.90). In addition, compared with the random assignment of travelers' destination based on the relative population size of states, countries whose GDP per capita was below the median indicated q = 2.5 (k = 0.01) to 2.8 (k = 0.90) times greater risk of yellow fever.

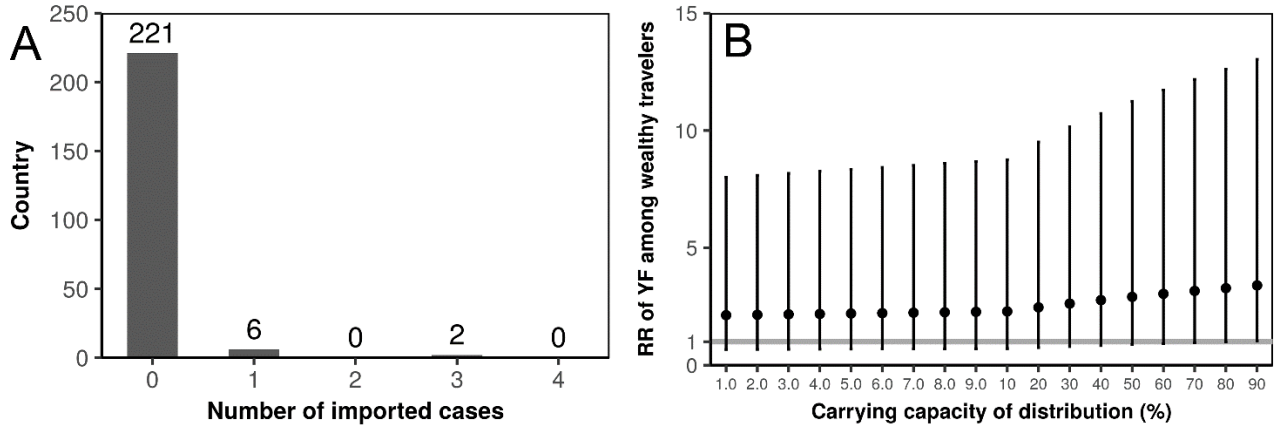

Figure 6. Risk of yellow fever among travelers visiting Brazil. **a** Observed distribution of number of imported cases of yellow fever from Brazil. As of May 8, 2018, 12 cases were diagnosed in 8 countries. Four or more imported cases were not reported in any country. **b** Sensitivity of relative risk of yellow fever among travelers to assumed maximum vaccination coverage (horizontal axis). Vertical axis represents relative risk of importation among countries whose GDP per capita was above the median compared with that of remaining countries. Filled circles represent maximum likelihood estimates, and whiskers extend to upper and lower 95% confidence intervals as computed from profile likelihood. Horizontal gray line indicates value of 1.0.

Discussion

Unlike the 2016–2017 epidemic in Brazil, which occurred primarily in the states of Minas Gerais and Espirito Santo, the 2017–2018 epidemic involved primarily São Paulo and Rio de Janeiro, which resulted in multiple international disseminations of imported cases. To identify the factors that contributed to this phenomenon and develop possible countermeasures, the distribution of imported cases from Brazil was investigated in the present study. Using a statistical model, we identified the risk of imported cases, jointly estimated the relative risk of travelers based on the extent of wealth (or GDP per capita), and compared the relative difference with the random assignment of travelers' destinations within Brazil. The results show that wealthier travelers were indicated 2.1–3.4 times greater risk of infection compared with the others. Moreover, among countries with the lower half of the GDP per capita, the risk was 2.5–2.8 times greater than that based on the assumption that the relative risk within Brazil is determined by the regional population size.

The two main contributions of this study are as follows: First, we showed that countries with a wealthier GDP per capita had a higher rate of infection. This finding is consistent with the fact that imported cases originated from a vacation locale in Ilha Grande, municipality of Angra do Reis, State of Rio de Janeiro (Ministerio da Saude, Brazil, 2018; Gossner et al, 2018). Furthermore, it indicates that travelers' local destination and behavior are likely to be key determinants of the heterogeneous risk of importing cases. Therefore, it is advisable to inform travelers of the ongoing geographic foci of transmission. If visits to tourist destinations with a history of imported cases are inevitable, then travelers are urged to receive vaccination in advance.

Second, we discovered that non-wealthy countries indicated 2.5–2.8 times greater risk of importing yellow fever cases compared with the typical modeling assumption (i.e., $q = 1.0$ in Eq. (10)) that the destination-specific risk of infection is proportional to the population size of the destination relative to the entire country. In Brazil, the major tourist destinations for international travelers are São Paulo and Rio de Janeiro. To precisely estimate the risk of infection among travelers, travel patterns in Brazil should be monitored more comprehensively. A significant challenge in achieving the precise estimation of risk in the future would be the quantification of

such risks on a finer spatial scale using limited mobility information among travelers.

This study exhibited four limitations: First, the notification of yellow fever cases was biased by the extent of the ascertainment. Hence, although we discovered that travelers from countries with a greater GDP per capita were at a greater risk of yellow fever, this finding only partially reflected the better ascertainment of cases in wealthier countries compared with the remaining countries. Second, we were unable to account for the spatial risk of infection on a finer scale. As of May 8, 2018, transmission has not been established within the city of Rio de Janeiro (Couto-Lima et al, 2017); hence, such risks must be communicated with greater precision using a risk map, as published elsewhere (Shearer et al, 2018; Garske et al, 2014; Hamlet et al, 2018; Nishiura et al, 2018). Third, vaccination coverage among travelers from countries without routine yellow fever immunization was assumed to be proportional to the GDP per capita. In the present study, our estimates were not sensitive to the ceiling of vaccination coverage, k; hence, the abovementioned assumption must be validated based on empirical observations in the future. Fourth, the lower confidence bound of our relative risk estimates was less than 1 (e.g., with k = 0.10, the lower 95% CI of a was 0.6), and the sample size was not substantial. This was due to the limited number of countries with imported yellow fever cases. Using a larger sample size in future follow-up studies would reduce the uncertainties and hence further support our conclusions.

The abovementioned future tasks should be considered to achieve a finer estimation of the infection risk among travelers. However, in our study, we successfully quantified the relative risk of infection based on the GDP per capita as well as compared it with the risk associated with the population-size-specific assumptions of travelers' destinations. Microgeographic information regarding imported cases should be effectively disseminated among travelers for communication and prevention purposes.

Acknowledgements

HN received funding support from the Japan Agency for Medical Research and Development, the Japan Science and Technology Agency (JST) CREST program (JPMJCR1413), the Telecommunication Advancement Foundation, and the Japan Society for the Promotion of Science (JSPS) KAKENHI 16KT0130 and 17H04701. The funders did not participate in the

study design, data collection and analysis, decision to publish, or manuscript preparation.

Chapter 2 was originally published in

Sakamoto Yohei, Takayuki Yamaguchi, Nao Yamamoto, Nishiura Hiroshi. Modeling the elevated risk of yellow fever among travelers visiting Brazil in 2018 Theoretical biology and medical Modeling 2018;15(9).

Conclusion

This study has developed mathematical models and risk assessments for two viral infections with different characteristics.

Chapter 1 provided an assessment of the risk of CMV among pregnant women in Japan. Data from the seroprevalence survey among pregnant women were analyzed as a function of time, and seropositivity among pregnant women was calculated by year. By fitting the computed probability to the observed seropositive data, we showed that the observed decline in the proportion of CMV-positive pregnant women mirrored the steadily declining force of infection over time. Owing to the elevated age at infection, pregnant women were exposed to a high risk of congenital CMV infections in Japan. Although routine testing for CMV infection in pregnant women is not currently recommended in Japan, the risk of infection during pregnancy may increase in the future, as shown in this study; hence, a system that can establish appropriate surveillance data should be developed.

Chapter 2 presented an evaluation of the risk of yellow fever about the outbreak in Brazil, 2018. Travelers from wealthier countries were at an elevated risk of yellow fever, thereby allowing us to speculate that travelers' local destination and behavior are likely to be key determinants of the heterogeneous risk of importation. Travelers should be informed of the ongoing geographic foci of transmission. If visits to tourist destinations with a history of imported cases are inevitable, then travelers are urged to receive vaccination in advance. For viral infections such as yellow fever, for which no effective drug treatment is available other than vaccines, it is necessary to accurately assess the risk, recommend vaccination, and educate people regarding behaviors that will expose them to the risk of infection.

The most common basic mathematical model that captures the epidemic dynamics of infectious diseases that are transmitted directly from person to person is called the SIR model. It divides the population into three compartments, susceptible, infectious, and removed/recovered, according to the stage of infection, and models the temporal changes in the state of infection. The SIR model and its analogs are characterized by high robustness and

can be easily extended and modified according to various situations and characteristics. The model in chapter 1 of this study is based on the SI model, which is an analog of the SIR model. These models can be applied not only to pandemic diseases such as SARS, MERS, and COVID-19, but also to infections that progress very slowly, such as HIV, and to infections that have different transmission routes from other infections, such as sexually transmitted diseases and mosquito-borne diseases. It has become common to fit these mathematical models to the observed data and estimate the parameters in recent years. By fitting these mathematical models to observed data, it has become possible to estimate the basic reproduction number (the number of secondary cases which one case would produce in a completely susceptible population) and the effective reproduction number (the expected number of secondary cases arising from a single primary case at calendar time t) in real-time. By estimating them, it has become possible to quantify the prevalence of infectious diseases, assess risks, make predictions, and objectively evaluate the effects of interventions. In addition, maximum likelihood estimation has been the most common parameter estimation method, but with the improvement of computer performance, Bayesian estimation represented by Markov Chain Monte Carlo method, and machine learning estimation methods are used and are expected to be further developed in the future.

However, sufficient observational and epidemiological data are not always available for all infectious diseases from the beginning. COVID-19, a global pandemic since 2020, initially lacked adequate observational and epidemiological data, but as a result of repeated epidemiological studies, including mathematical models, a reliable model has been constructed. When constructing mathematical models in a situation with insufficient data, it is essential to ensure their validity from clinical, biological, or social medical perspectives. The publication of such models will lead to the construction of appropriate surveillance.

In Japan, sufficient epidemiological data on congenital infections such as CMV and imported infections are not yet available, and these infections' prevalence and risk assessment are not sufficiently understood. I hope that this study will lead to appropriate surveillance for these infections in the future.

Acknowledgements

First, I would like to express my heartfelt gratitude to Prof. Nishiura for his persistent guidance at the beginning when I did not know statistics, mathematics, or English and had never written a paper before. I am very fortunate that Prof. Nishiura, a leading researcher in the mathematical modeling of infectious diseases, took the time to mentor me out of his busy schedule. I hope he will continue to play an active role in the field of epidemiology of infectious diseases. I would also like to thank Nao Yamamoto and Takayuki Yamaguchi for writing paper with me and always helping me, and Yusuke Asai and Shinya Tsuzuki for always giving me appropriate advice and knowledge. And finally, I would like to thank my wife and son for always supporting and encouraging me.

Conflicts of interest

The author declares no conflict of interest.

References

Almeida, L.N., Azevedo, R.S., Amaku, M., and Massad, E. (2001). Cytomegalovirus seroepidemiology in an urban community of São Paulo, Brazil. Rev. Saude. Publica. *35*, 124–129.

Anderson, R. M. and May, R. M.（1982）. Directly transmitted infectious diseases: Control by vaccination. Science. *215*, 1053–1060.

Azevedo, R.S., and Amaku, M. (2011). Modelling immunization strategies with cytomegalovirus vaccine candidates. Epidemiol. Infect. *139*, 1818–1826.

Azuma, H., Takanashi, M., Kohsaki, M., Sato, H., Ishimura, F., and Yamada, H. (2010). Cytomegalovirus seropositivity in pregnant women in Japan during 1996-2009. Journal of Japan Society of Perinatal and Neonatal Medicine *46*, 1273–1279.

Bollaerts, K., Riera-Montes, M., Heininger, U., Hens, N., Souverain, A., Verstraeten, T., and Hartwig, S. (2017). A systematic review of varicella seroprevalence in European countries before universal childhood immunization: deriving incidence from seroprevalence data. Epidemiol. Infect. *145*, 2666–2677.

Boven, M., Kassteele, J., Korndewal, M.J., Dorp, C.H., Kretzschmar, M., Klis, F., Melker, H.E., Vossen, A.C., and Baarle, D. (2017). Infectious reactivation of cytomegalovirus explaining age- and sex-specific patterns of seroprevalence. PLoS Comput Biol. *13*: e1005719.

Central Intelligence Agency. (2017). The World Factbook. Country Comparison: GDP-Per Capita (PPP). https://www.cia.gov/the-world-factbook/field/real-gdp-per-capita/country-comparison (Accessed: 31 Oct 2021)

Colugnati, F.A., Staras, S.A., Dollard, S.C., and Cannnon, M.J. (2007). Incidence of cytomegalovirus infection among the general population and pregnant women in the United States. BMC Infect Dis. *7*, 71.

Couto-Lima, D., Madec, Y., Bersot, M.I., Campos, S.S., Motta, M.A., Santos, F.B.D., Vazeille, M., Vasconcelos, P.F.D.C., Lourenço-de-Oliveira, R., and Failloux, A.B. (2017). Potential risk of re-emergence of urban transmission of yellow fever virus in Brazil facilitated by competent Aedes populations. Sci Rep. *7*, 4848.

Dexheimer, Paploski, I.A., Souza, R.L., Tauro, L.B., Cardoso, C.W., Mugabe, V.A., Pereira, Simões, Alves, A.B., Jesus, Gomes, J., Kikuti, M., Campos, G.S., Sardi, S., et al. (2018). Epizootic outbreak of yellow fever virus and risk for human disease in Salvador, Brazil. Ann Intern Med. *168*, 301–302.

Dietz, K and Heesterbeek, H. (2002). Daniel Bernoulli's epidemiological model revisited. Math Biosci. *180*, 1-21.

Dietz, K. (1988). The first epidemic model: a historical note on P.D. EN'KO. Aust. J. Stat. *30*, 56-65.

Dorigatti, I., Hamlet, A., Aguas, R., Cattarino, L., Cori, A., Donnelly, C.A., Garske, T., Imai, N., and Ferguson, N.M. (2017). International risk of yellow fever spread from the ongoing outbreak in Brazil, December 2016 to May 2017. Euro Surveill. *22*, 30572.

Dowd, J.B., Aiello, A.E., and Alley, D.E. (2009). Socioeconomic disparities in the seroprevalence of cytomegalovirus infection in the US population: NHANES III. Epidemiol. Infect. *137*, 58–65.

Fang, F.Q., Fan, Q. S., Yang, Z.J., Peng, Y.B., Zhang, L., Mao, K.Z., Zhang, Y., and Ji, Y.H. (2009). Incidence of Cytomegalovirus Infection in Shanghai, China. Clin. Vaccine. Immunol. *16*, 1700–1703.

Fernandes, G.C.V.R., Azevedo, R.S., Amaku, M., Yu, A.L.F, and Massad, E. (2009). Seroepidemiology of Toxoplasma infection in a metropolitan region of Brazil. Epidemiol. Infect. *137*: 1809–1815.

Fernandes, N.C.C.A., Cunha, M.S., Guerra, J.M., Réssio, R.A., Cirqueira, C.D.S., Iglezias, S.D., de Carvalho, J., Araujo, E.L.L., Catão-Dias, J.L., and Díaz-Delgado, J. (2017). Outbreak of yellow fever among nonhuman Primates, Espirito Santo, Brazil, 2017. Emerg Infect Dis. *23*, 2038–2041.

Garske, T., Van Kerkhove, M.D., Yactayo, S., Ronveaux, O., Lewis, R.F., Staples, J.E., Perea, W., and Ferguson, N.M. (2014). Yellow fever expert committee. Yellow fever in Africa: estimating the burden of disease and impact of mass vaccination from outbreak and serological data. PLoS Med. *11*, e1001638.

Glasser, J., Meltzer, M. and Levin, B. (2004). Mathematical modeling and public policy: responding to health crises. *Emerg Infect Dis*. 10, 2050–2051.

Gossner, C.M., Haussig, J.M., de Saint, Lary, C.B., Aaslav, K.K., Schlagenhauf, P., and Sudre, B. (2018). Increased risk of yellow fever infections among unvaccinated European travellers due to ongoing outbreak in Brazil, July 2017 to March 2018. Euro Surveill. *23*, 18–00106.

Griffiths, P.D., McLean, A., and Emery, V.C. (2001). Encouraging prospects for immunisation against primary cytomegalovirus infection. Vaccine *19*, 1356–1362.

Hamlet, A., Jean, K., Perea, W., Yactayo, S., Biey, J., Van Kerkhove, M., Ferguson, N., and Garske, T. (2018). The seasonal influence of climate and environment on yellow fever transmission across Africa. PLoS Negl Trop Dis. *12*, e0006284.

Hirota, K. (1992). Prospective study on maternal, intrauterine, and perinatal infections with cytomegalovirus in Japan during 1976-1990. J. Med. Virol. *37*, 303–306.

Hogea, C., Dieussaert, I., Effelterre T.V., Guignard, A., and Mols, J. (2015). A dynamic transmission model with age-dependent infectiousness and reactivation for cytomegalovirus in the United States: Potential impact of vaccination strategies on congenital infection. Hum. Vaccine. Immunother. 11: 1788–1802.

Johansson, M.A., Vasconcelos, P.F., and Staples, J.E. (2014). The whole iceberg: estimating the incidence of yellow fever virus infection from the number of severe cases. Trans R Soc Trop Med Hyg. *108*, 482–487.

Kafatos, G., Andrews, N.J., McConway, K.J., Maple, P.A.C., Brown, K., and Farrington, C.P. (2016). Is it appropriate to use fixed assay cut-offs for estimating seroprevalence? Epidemiol. Infect. *144*: 887–895.

Kenneson, A.and Cannon, M.J. (2007). Review and meta-analysis of the epidemiology of congenital cytomegalovirus (CMV) infection. Rev. Med. Virol. *17*, 253–276.

Kermack, W.O. and Mckendrick, A.G. (1927). Contributions to the mathematical theory of epidemics-I. Proc R Soc Lond B Biol Sci. *115*, 700-721.

Lanzieri, T.M., Bialek, S.R., Ortega-Sanchez, I.R., and Gambhir, M. (2014). Modeling the potential impact of vaccination on the epidemiology of congenital cytomegalovirus infection. Vaccine. *32*: 3780–3786.

Ministerio da Saude, Brazil. (2018). Monitoramento do Período Sazonal da Febre Amarela. Brasil – 2017/2018. 8 May 2018. INFORME N25. São Paulo: Ministerio da Saude; 2018. http://portalarquivos2.saude.gov.br/images/pdf/2018/maio/09/Informe-FA.pdf (Accessed: 31 Oct 2021)

Ministry of Health, Labour and Welfare, Japan (MHLW). (1980-2009). Vital Statistics. Tokyo: Ministry of Health, Labour and Welfare. https://www.e-stat.go.jp/en/stat-search/files?page=1&toukei=00450011&tstat=000001028897. (Accessed: 31 Oct 2021)

Monath, T.P. (2001). Yellow fever: an update. Lancet Infect Dis. *1*, 11–20.

Moreira-Soto, A., Torres, M.C., Lima, de Mendonça, M.C., Mares-Guia, M.A., Dos, Santos, Rodrigues, C.D., Fabri, A.A., Dos, Santos, C.C., Machado, Araújo, E.S., Fischer, C., Ribeiro, Nogueira, R.M., et al. (2018). Evidence for multiple sylvatic transmission cycles during the 2016-2017 yellow fever virus outbreak, Brazil. Clin Microbiol Infect. *24*, 1019.

Mossong, J., Hens, N., Friederichs, V., Davidkin, I., Broman, M., Litwinska, B., Siennicka, J., Trzcinska, A., Damme, P., Beutels, P., et al. (2008). Parvovirus B19

infection in five European countries: seroepidemiology, force of infection and maternal risk of infection. Epidemiol. Infect. *136*: 1059–1068.

Mossong, J., Putz, L., and Schneider, F. (2004). Seroprevalence and force of infection of varicella-zoster virus in Luxembourg. Epidemiol. Infect. *132*: 1121–1127.

Nishiura, H., Tsuzuki, S., and Asai, Y. (2018). Forecasting the size and peak of cholera epidemic in Yemen, 2017. Future Microbiol. *13*, 399–402.

Ogawa, H., Suzutani, T., Baba Y., Kayano, S., Nozawa, N., Ishibashi, K., Fujieda, K., Inoue, N., and Oomori, K. (2007). Etiology of severe sensorineural hearing loss in children: in- dependent impact of congenital cytomegalovirus infection and GJB2 mutations. J. Infect Dis. *195*, 782–788.

Pan American Health Organization. (2018). Yellow fever. Epidemiological update on 12 January 2018. Washington D.C.: Pan American Health Organization;2018. https://www.paho.org/hq/index.php?option=comcontent&view=article&id=14043%3A12 https://www3.paho.org/hq/index.php?option=com_docman&view=download&category_slug=yellow-fever-2194&alias=43320-12-january-2018-yellow-fever-epidemiological-update-320&Itemid=270&lang=en (Accessed: 31 Oct 2021)

Possas, C., Martins, R.M., Oliveira, R.L., and Homma, A. (2018). Urgent call for action:avoiding spread and re-urbanisation of yellow fever in Brazil. Mem Inst Oswaldo Cruz. *113*, 1–2.

Rieder, H. (2005). Annual risk of infection with Mycobacterium tuberculosis. Eur. Respir. J. *25*: 181–185.

Shearer, F.M., Longbottom, J., Browne, A.J., Pigott, D.M., Brady, O.J., Kraemer, M.U.G., Marinho, F., Yactayo, S., de Araújo, V.E.M., da Nóbrega, A.A., et al. (2018). Existing and potential infection risk zones of yellow fever worldwide: a modelling analysis. Lancet Global Health. *6*, e270–278.

Shearer, F.M., Moyes, C.L., Pigott, D.M., Brady, O.J., Marinho, F., Deshpande, A., Longbottom, J., Browne, A.J., Kraemer, M.U.G., O'Reilly, K.M., et al. (2017). Global yellow fever vaccination coverage from 1970 to 2016: an adjusted retrospective analysis. Lancet Infect Dis. *17*, 1209–1217.

Stagno, S., and Whitley, R.J. (1985). Herpesvirus infections of pregnancy. Part I: Cytomegalovirus and Epstein-Barr virus infections. N. Engl. J. Med. *313*, 1270–1274.

Taniguchi, K., Watanabe, N., Sato, A., Jwa, S.C., Suzuki, T., Yamanobe, Y., Sago, H., and Kozuka, K. (2014). Changes in cytomegalovirus seroprevalence in pregnant Japanese women-a 10 year single center study. J. Clin. Virol. *59*, 192–194.

Tsuzuki, S., Lee, H., Miura, F., Chan, Y.H., Jung, S.M., Akhmetzhanov, A.R., and

Nishiura, H. (2017). Dynamics of the pneumonic plague epidemic in Madagascar, August to October 2017. Euro Surveill. *22*, 17-00710.

Vyse, A.J., Hesketh, L.M., and Pebody, R.G. (2009). The burden of infection with cytomegalovirus in England and Wales: how many women are infected in pregnancy? Epidemiol. Infect. *137*: 526–533.

Weigand, G. YELLOW FEVER - AMERICAS (24): GERMANY ex BRAZIL (RIO DE JANEIRO). (2018). ProMED-mail, 27 March 2018. https://www.promedmail.org/post/20180327.5714395 (Accessed: 31 Oct 2021)

Wisseman, C.L., Sweet, B.H., Kitaoka, M., and Tamiya, T. (1962). Immunological studies with group B arthropod-borne viruses. I. Broadened neutralizing antibody spectrum induced by strain 17D yellow fever vaccine in human subjects previously infected with Japanese encephalitis virus. Am J Trop Med Hyg. *11*, 550–61.

World Health Organization. (2018a). Disease outbreak news on 22 January 2018. Yellow fever – Brazil. Geneva: World Health Organization. https://www.who.int/emergencies/disease-outbreak-news/item/22-january-2018-yellow-fever-brazil-en (Accessed: 31 Oct 2021)

World Health Organization. (2018b). Disease outbreak news on 27 February 2018. Yellow fever – Brazil. Geneva: World Health Organization. https://www.who.int/emergencies/disease-outbreak-news/item/27-february-2018-yellow-fever-brazil-en (Accessed: 31 Oct 2021)

World Health Organization. (2018c). Disease outbreak news on 9 March 2018. Yellow fever – Brazil. Geneva: World Health Organization. https://www.who.int/emergencies/disease-outbreak-news/item/09-march-2018-yellow-fever-brazil-en (Accessed: 31 Oct 2021)

World Tourism Organization (UNWTO). Yearbook of Tourism Statistics dataset. (2017). Brazil. Geneva. https://www.unwto.org/global/publication/yearbook-tourism-statistics-data-2013-2017-2019-edition (Accessed: 31 Oct 2021)